AMERICAN SOCIETY FOR MICROBIOLOGY | Applied and Environmental Microbiology®

GENETICS AND MOLECULAR BIOLOGY

The Small RNAs PA2952.1 and PrrH as Regulators of Virulence, Motility, and Iron Metabolism in *Pseudomonas aeruginosa*

Shannon R. Coleman,[a] Manjeet Bains,[a] Maren L. Smith,[a] Victor Spicer,[b] Ying Lao,[b] Patrick K. Taylor,[a] Neeloffer Mookherjee,[b] Robert E. W. Hancock[a]

[a]Center for Microbial Diseases and Immunity Research, Department of Microbiology and Immunology, University of British Columbia, Vancouver, Canada
[b]Manitoba Center for Proteomics & Systems Biology, Department of Internal Medicine, University of Manitoba, Winnipeg, Canada

ABSTRACT *Pseudomonas aeruginosa* is a Gram-negative opportunistic pathogen that undergoes swarming motility in response to semisolid conditions with amino acids as a nitrogen source. With a genome encoding hundreds of potential intergenic small RNAs (sRNAs), *P. aeruginosa* can easily adapt to different conditions and stresses. We previously identified 20 sRNAs that were differentially expressed (DE) under swarming conditions. Here, these sRNAs were overexpressed in strain PAO1 and were subjected to an array of phenotypic screens. Overexpression of the PrrH sRNA resulted in decreased swimming motility, whereas a Δ*prrH* mutant had decreased cytotoxicity and increased pyoverdine production. Overexpression of the previously uncharacterized PA2952.1 sRNA resulted in decreased swarming and swimming motilities, increased gentamicin and tobramycin resistance under swarming conditions, and increased trimethoprim susceptibility. Transcriptome sequencing (RNA-Seq) and proteomic analysis were performed on the wild type (WT) overexpressing PA2952.1 compared to the empty vector control under swarming conditions, and these revealed the differential expression (absolute fold change [FC] $\geq$ 1.5) of 784 genes and the differential abundance (absolute FC $\geq$ 1.25) of 59 proteins. Among these were found 73 transcriptional regulators, two-component systems, and sigma and anti-sigma factors. Downstream effectors included downregulated pilus and flagellar genes, the upregulated efflux pump MexGHI-OpmD, and the upregulated *arn* operon. Genes involved in iron and zinc uptake were generally upregulated, and certain pyoverdine genes were upregulated. Overall, the sRNAs PA2952.1 and PrrH appeared to be involved in regulating virulence-related programs in *P. aeruginosa*, including iron acquisition and motility.

IMPORTANCE Due to the rising incidence of multidrug-resistant (MDR) strains and the difficulty of eliminating *P. aeruginosa* infections, it is important to understand the regulatory mechanisms that allow this bacterium to adapt to and thrive under a variety of conditions. Small RNAs (sRNAs) are one regulatory mechanism that allows bacteria to change the amount of protein synthesized. In this study, we overexpressed 20 different sRNAs in order to investigate how this might affect different bacterial behaviors. We found that one of the sRNAs, PrrH, played a role in swimming motility and virulence phenotypes, indicating a potentially important role in clinical infections. Another sRNA, PA2952.1, affected other clinically relevant phenotypes, including motility and antibiotic resistance. RNA-Seq and proteomics of the strain overexpressing PA2952.1 revealed the differential expression of 784 genes and 59 proteins, with a total of 73 regulatory factors. This substantial dysregulation indicates an important role for the sRNA PA2952.1.

KEYWORDS *Pseudomonas aeruginosa*, antibiotic resistance, proteomics, small RNAs, swarming motility, transcriptomics, virulence

Citation Coleman SR, Bains M, Smith ML, Spicer V, Lao Y, Taylor PK, Mookherjee N, Hancock REW. 2021. The small RNAs PA2952.1 and PrrH as regulators of virulence, motility, and iron metabolism in *Pseudomonas aeruginosa*. Appl Environ Microbiol 87:e02182-20. https://doi.org/10.1128/AEM.02182-20.

Editor Maia Kivisaar, University of Tartu

Address correspondence to Robert E. W. Hancock, bob@hancocklab.com.

Received 8 September 2020
Accepted 3 November 2020
Accepted manuscript posted online 6 November 2020
Published 15 January 2021

Pseudomonas aeruginosa, a Gram-negative rod-shaped proteobacterium, is an opportunistic pathogen of humans. Responsible for morbidity and mortality in diverse diseases such as cystic fibrosis, pneumonia, nosocomial infections, ear and urinary tract infections, bacterial keratitis, and chloronychia (1–4), *P. aeruginosa* is a rising global threat due to the emergence of multidrug-resistant (MDR) strains. Additionally, *P. aeruginosa* also possesses intrinsic resistance due to its low outer membrane permeability and the presence of numerous multidrug efflux systems (5, 6). Using its large (5- to 7-Mbp) genome, *P. aeruginosa* is able to adapt to and thrive in a variety of different environments and growth states.

Motility is an important adaptation for bacteria to spread in the environment, colonize new niches, and infect hosts. *P. aeruginosa* exhibits several forms of motility, including swimming (or planktonic movement using flagella), twitching (via extension and retraction of the type IV pilus), surfing (a surface motility dependent on the presence of mucin) (7), and swarming (8). In *P. aeruginosa*, swarm cells are approximately twofold elongated and may acquire an extra polar flagellum (8). Groups of swarm cells raft together in a multicellular movement over moist surfaces of intermediate viscosity and manifest on a macroscopic scale as tendrils or flares of various thicknesses branching from the central colony. In *P. aeruginosa*, swarming relies on both flagella and type IV pili, as well as on the secretion of surfactant rhamnolipids (8, 9). Previous studies have shown that swarming cells are resistant to multiple antibiotic classes (10–12).

Coupling a large genome with a high percentage of transcriptional regulators (roughly 10%), *P. aeruginosa* also has considerable genetic and regulatory potential to adapt to different conditions, such as different types of surfaces or antibiotic treatment. In addition, hundreds of regulatory small RNAs (sRNAs), interspersed throughout the genome, have been predicted (13, 14). These noncoding regulatory elements allow for rapid regulation, typically through posttranscriptional modification (often translational repression) (15). Additionally, some sRNAs can influence the degradation of or increase stability of mRNAs (16, 17). sRNAs can interact with regions near the ribosome binding site to inhibit or enhance translation (18–20). A chaperone facilitating sRNA-mRNA interactions, such as Hfq, is often required (21). Lastly, sRNAs can also act as a sponge to sequester regulatory proteins or interact with proteins to modulate their activity (16, 19, 21).

A 2018 study examined the expression of intergenic sRNAs and found that 31 species were differentially expressed (DE) under swarming and/or biofilm conditions (22). Most of the 20 sRNAs that were differentially expressed under swarming conditions were previously uncharacterized, except for PrrH, RsmY, and SrbA. A previous study showed that deleting SrbA had an effect on biofilm formation and virulence in a *Caenorhabditis elegans* infection model, but little else is known regarding this sRNA (23). More is known about the sRNAs RsmY and RsmZ, which are partially redundant and act by sequestering the posttranscriptional regulator RsmA, causing diverse effects on virulence, including the type III and VI secretion systems (T3SS and T6SS), quorum sensing (QS), biofilm formation, iron homeostasis, and type IV pili (16, 24, 25).

The two tandem and highly homologous PrrF sRNAs PrrF1 and PrrF2 are involved in iron homeostasis and virulence *in vivo*, and work in conjunction with the RNA-binding protein Hfq (16, 26). The entire PrrF1-PrrF2 region can also be transcribed as a whole, referred to as PrrH (16). Under iron-replete conditions, the repressor Fur binds iron and represses PrrH, whereas PrrH represses or spares the use of iron under iron-limiting conditions (16). Interestingly, PrrH also represses the expression of AntR, a positive regulator of genes that convert anthranilate into catechol (16). When AntR is repressed, anthranilate is instead channeled into the *Pseudomonas* quinolone signal (PQS) system, resulting in the increased expression of virulence factors (16). The sRNA CrcZ competes with PrrH for binding to Hfq and can act as a sponge, since CrcZ has a higher affinity for Hfq than does PrrH (16, 27).

Here, we probed the role of sRNAs in adaptive behaviors in *P. aeruginosa* by cloning and overexpressing sRNAs that were differentially expressed under swarming conditions.

The overexpressing strains were examined in phenotypic assays for motility, cytotoxicity, and adherence. The strain overexpressing PA2952.1 showed differences in several assays (decreased motility and altered antibiotic susceptibility) and was therefore selected for further analysis. To investigate the effects mediated by the sRNA PA2952.1 in more detail, transcriptome sequencing (RNA-Seq) and proteomic analysis were performed, revealing the differential abundance of 784 transcripts and 59 proteins, including motility, antibiotic resistance, and metal uptake genes.

RESULTS

Phenotypic screens of sRNA overexpression strains. Putative sRNAs were identified by RNA-Seq in two studies (13, 14). Our lab confirmed the expression of some of the sRNAs by RNA-Seq and quantitative reverse transcriptase PCR (qRT-PCR) (22). Furthermore, we investigated the differential expression of these sRNAs in the context of two adaptive phenotypes, swarming motility and biofilm formation, and showed that 30 of 31 sRNAs showed differential expression under one or both conditions (22). Focusing on swarming motility, sRNA species that were differentially expressed under swarming conditions (22) were cloned to enable overexpression, as sRNAs often have inhibitory functions. To determine which region or orientation might result in a phenotype, some of these sRNAs were cloned in two orientations (PA0805.1 and PA0805.1a; PA1091.1a and b; PA3159.1a and b; and PA4656.1a and b), or different regions were cloned (PA2952.1W, an overlapping version of PA2952.1; PA14sr120, a shorter version of PA0805.1) (13, 14, 22). A total of 21 constructs were made in the arabinose-inducible pHERD20T vector and transformed into the PAO1 H103 wild type (WT) by electroporation. One of these, PA0805.1, was previously described (28) and is not discussed further in this study.

At the time of the assay, arabinose was added to induce sRNA expression. Overexpression strains were confirmed to have no growth defects (see Fig. S1A in the supplemental material). Next, overexpression strains were screened for swarming, swimming, and twitching (Fig. 1). Strains were also screened for adherence to polystyrene, but showed little difference in this assay (see Fig. S3 in the supplemental material).

The results for swarming and swimming motilities correlated well for some strains in these experiments (Fig. 1). The overexpression strain PA14sr120 showed swarming and swimming motilities that were reduced to 81% $\pm$ 6% and 65% $\pm$ 2% of those of the WT containing the empty cloning vector (EV) (Fig. 1). The PA2952.1 overexpression strain showed motility that was reduced to 69% $\pm$ 3% and 43% $\pm$ 4% for swarming and swimming, respectively (Fig. 1). Swarming for the PA2952.1-overexpressing strain, measured as a percentage of WT EV area, was 50% $\pm$ 3%. The PA1091.1b-overexpressing strain showed a reduction in swarming motility to 80% $\pm$ 2% of WT EV levels (Fig. 1). Interestingly, overexpression of PrrH resulted in substantially reduced swimming (to 28% $\pm$ 3% of WT EV levels), but no change in swarming motility (Fig. 1). Overexpression strains were also screened for twitching motility but showed no significant difference (Fig. 1). Sample colonies showing partial reductions in motility are shown in Fig. 2. It is of note that the swarming pattern shown here is different from the dendritic pattern of strain PA14 (9), because swarming is highly dependent on the strain used and on medium composition.

The sRNA overexpression strains were also screened for cytotoxicity against human bronchial epithelial cells (HBE), with and without arabinose. Few significant differences were found amongst the strains (data not shown), except for PA2952.1 and PrrH. In the absence of arabinose, the strain overexpressing PA2952.1 showed cytotoxicity that was reduced by 36.4% compared to WT levels; however, the PA2952.1-overexpressing strain, compared to WT EV with 1% arabinose, was not significantly different (Fig. 3A).

PA2952.1 and PrrH were overexpressed robustly, and overexpression of PrrH influenced the expression of PA2952.1. To investigate the expression of sRNAs from the vector pHERD20T, and to determine whether sRNAs were overexpressed in the absence of arabinose, quantitative reverse transcriptase PCR (qRT-PCR) was performed

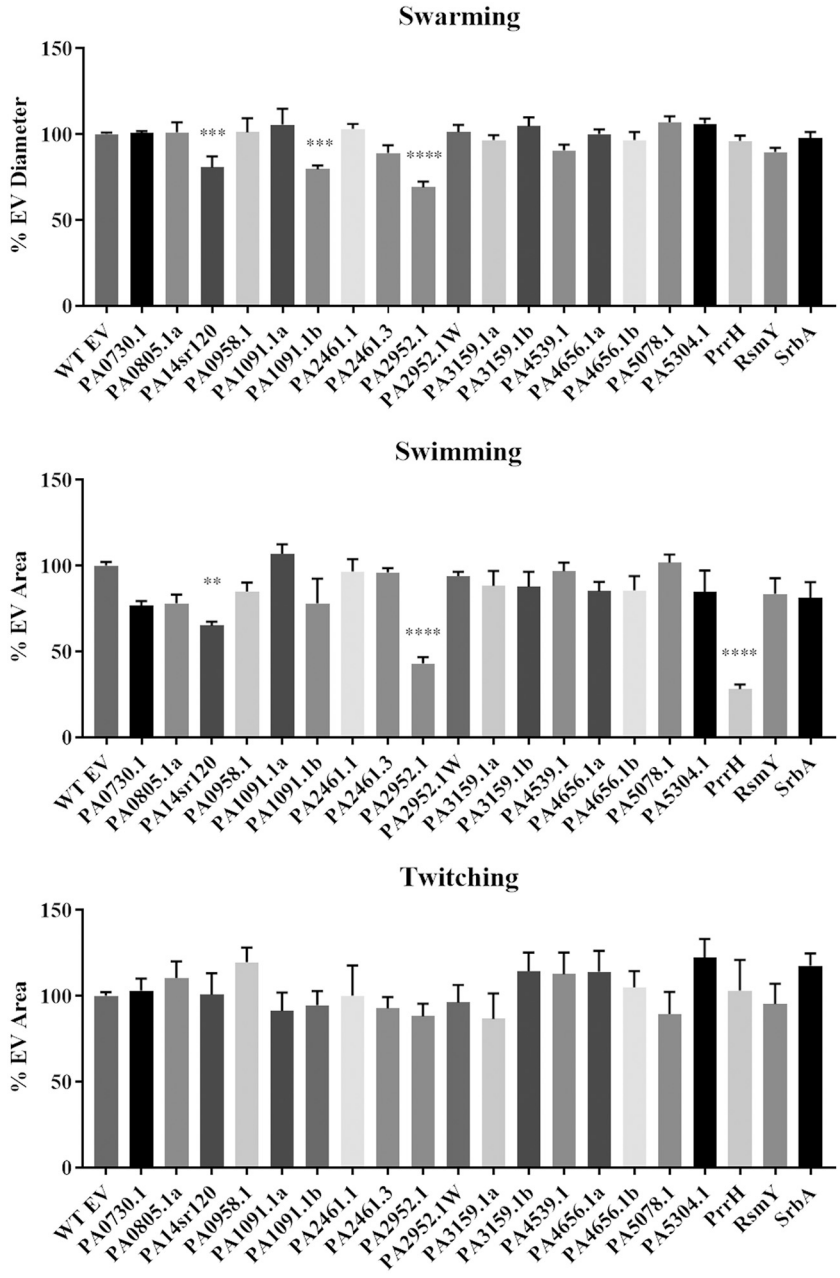

FIG 1 Motility screen of sRNA overexpression strains revealed that the overexpression of certain small RNAs (sRNAs) altered motility. 1% arabinose was used to induce expression, and statistically significant differences from the wild type (WT) carrying empty cloning vector (EV) were determined using one-way analysis of variance (ANOVA). Statistical significance is indicated by ** ($0.001 < P \leq 0.01$), *** ($0.0001 < P \leq 0.001$), and **** ($P \leq 0.0001$). $n \geq 3$.

under swarming conditions by comparing the two overexpression strains, PA2952.1 and PrrH, to the WT EV strain. Results indicated that both sRNAs overexpressed robustly from pHERD20T in the presence of arabinose (see Table S1 in the supplemental material). In the absence of arabinose, PA2952.1 and PrrH were also significantly overexpressed from pHERD20T, but to a much lesser extent than that with arabinose. Interestingly, overexpression of PrrH significantly affected the expression of PA2952.1, indicating a potential connection between the two sRNAs (Table S1).

PrrH played a role in cytotoxicity and pyoverdine production. The sRNA PrrH, encompassing the two adjacent and highly homologous sRNAs PrrF1 and PrrF2 (26), also played a role in cytotoxicity (Fig. 3B). When PrrH was overexpressed at low levels

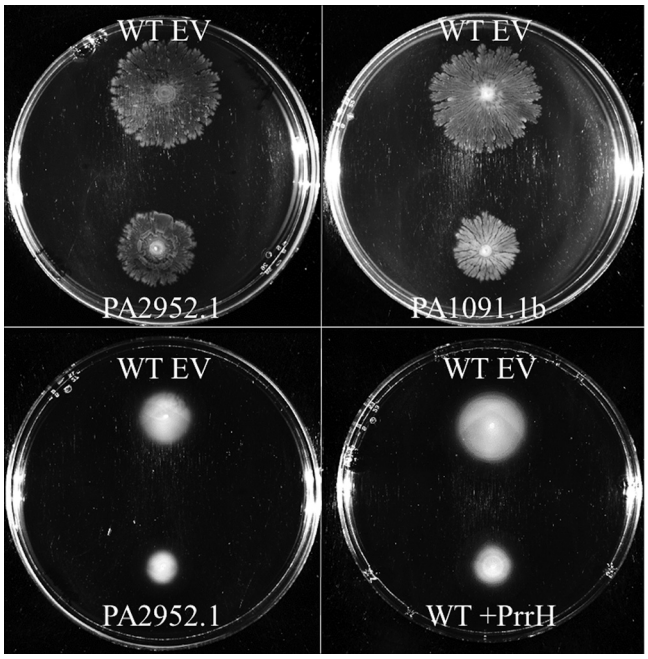

FIG 2 Overexpression of certain sRNAs led to partial reductions in swarming (top) and swimming (bottom) motilities. $n \geq 3$.

(0% arabinose), the cytotoxicity of the WT overexpressing PrrH (WT+PrrH) was reduced by 40.2% compared to WT levels. In the absence of arabinose, a Δ*prrH* deletion mutant showed even lower levels of cytotoxicity (reduced by 68.9%), which was partially complemented (to 53.7% of WT levels) when the sRNA was reintroduced on the uninduced pHERD20T plasmid (Fig. 3B). The fact that both overexpression and deletion of PrrH led to decreased cytotoxicity is counterintuitive and is not fully understood at the current time. However, this phenomenon is not unprecedented and could be explained by regulatory loops or threshold effects (29, 30). Threshold effects arise from a requirement of a specific level of sRNA to achieve the wild-type phenotype. Any departure from this level (increase or decrease) disrupts normal processes, resulting in a defective phenotype. Regulatory loops are another possibility to consider. For example, if PrrH

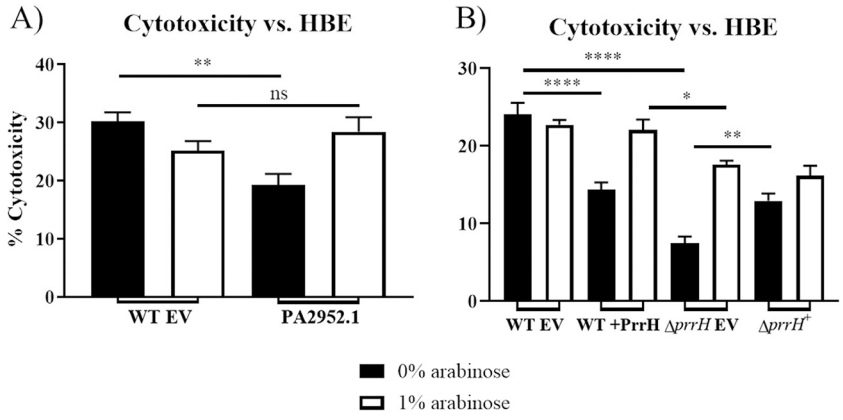

FIG 3 Cytotoxicity phenotypes of sRNA overexpression strains in the presence or absence of arabinose. Effects of overexpressing PA2952.1 compared to WT containing the empty cloning vector (A), and deletion, overexpression, and complementation of *prrH* compared to that in WT EV (B). Statistically significant differences were determined by one-way ANOVA. Percent cytotoxicity was assessed by the lactate dehydrogenase (LDH) assay and calculated relative to a Triton-X control. Statistical significance is indicated by * ($0.01 < P \leq 0.05$), ** ($0.001 < P \leq 0.01$), *** ($0.0001 < P \leq 0.001$), and **** ($P \leq 0.0001$). $n \geq 3$.

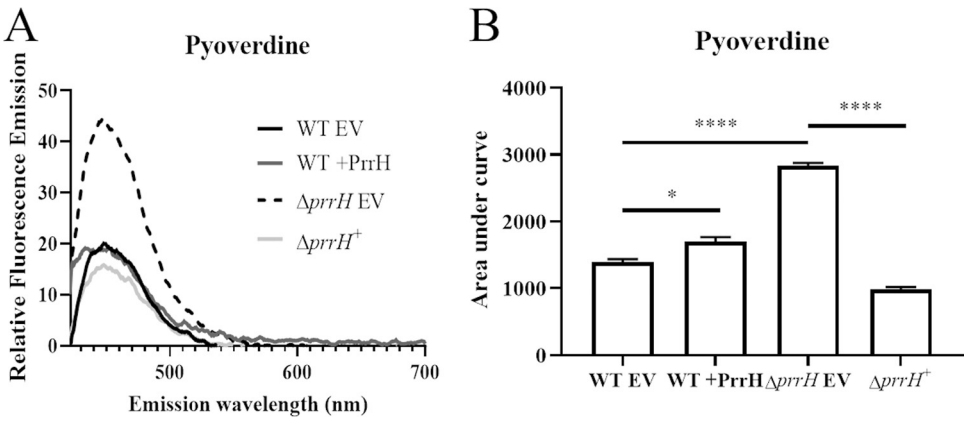

FIG 4 The Δ*prrH* deletion mutant showed increased production of pyoverdine. (A) Mean fluorescent emission peaks from the four strains. (B) Area under the curve of each peak was calculated for $n = 3$ in GraphPad Prism, and statistically significant differences were determined by ANOVA. Statistical significance is indicated by * ($0.01 < P \leq 0.05$) and **** ($P \leq 0.0001$).

negatively regulated its own expression, overexpressing PrrH could lead to the same result as deleting PrrH. Lastly, it is also possible that although the cytotoxicity phenotypes of the deletion and overexpression strains appeared similar, the phenotypes might have resulted from different gene expression programs in the two strains.

Interestingly, in the presence of arabinose, the cytotoxicity phenotypes were minimized, and only the change in cytotoxicity due to the deletion of PrrH was significantly different and could not be complemented by overexpression of PrrH (Fig. 3B). Expression of PrrH at a specific (i.e., lower) level may therefore be required for complementation. Growth curves performed in Dulbecco's modified Eagle's medium (DMEM) also showed no significant difference between strains (Fig. S1B).

The Δ*prrH* deletion mutant also had a greater than twofold increase in levels of pyoverdine production (Fig. 4). This phenotype was restored back to WT levels by complementation. The strain overexpressing PrrH, however, showed no difference compared to the WT EV isolate (Fig. 4).

Overexpression of sRNAs altered antibiotic susceptibility under swarming conditions. We considered whether some of the sRNAs might play a role in swarming-mediated antibiotic resistance (12). The sRNA PA2952.1, which inhibited swarming and swimming (Fig. 2), also showed altered antibiotic susceptibility under swarming conditions using a previously described method (12). PA2952.1 overexpression at low levels led to resistance to both tobramycin and gentamicin in both the absence (Fig. 5A) and presence of inducer arabinose (see Fig. S4 in the supplemental material, showing a milder phenotype due to the background effects of PA2952.1 overexpression on swarming motility). We confirmed that PA2952.1 was resistant to tobramycin by performing kill curves and showed that swarm cells overexpressing PA2952.1 had increased viability compared to that of WT EV during tobramycin treatment (see Fig. S5 in the supplemental material). Interestingly, no difference was observed under swimming conditions, indicating that the tobramycin phenotype might be specific to the swarm state (Fig. S5). In contrast, at higher levels of PA2952.1 expression (induced with 1% arabinose), increased susceptibility to trimethoprim was observed under swarming conditions (Fig. 5B). No major difference in the MIC to either antibiotic was observed in standard microdilution assays (see Table S2 in the supplemental material); however, subinhibitory concentrations of trimethoprim specifically inhibited the growth of the PA2952.1 overexpression strain in the presence of 1% arabinose (see Fig. S6 in the supplemental material).

Overexpression of the sRNA PA14sr120 at low levels resulted in resistance to tobramycin under swarming conditions (Fig. 5C). Similar to the observations made for PA2952.1, overexpression of PA1091.1b at high levels resulted in increased trimethoprim susceptibility under swarming conditions (Fig. 5D).

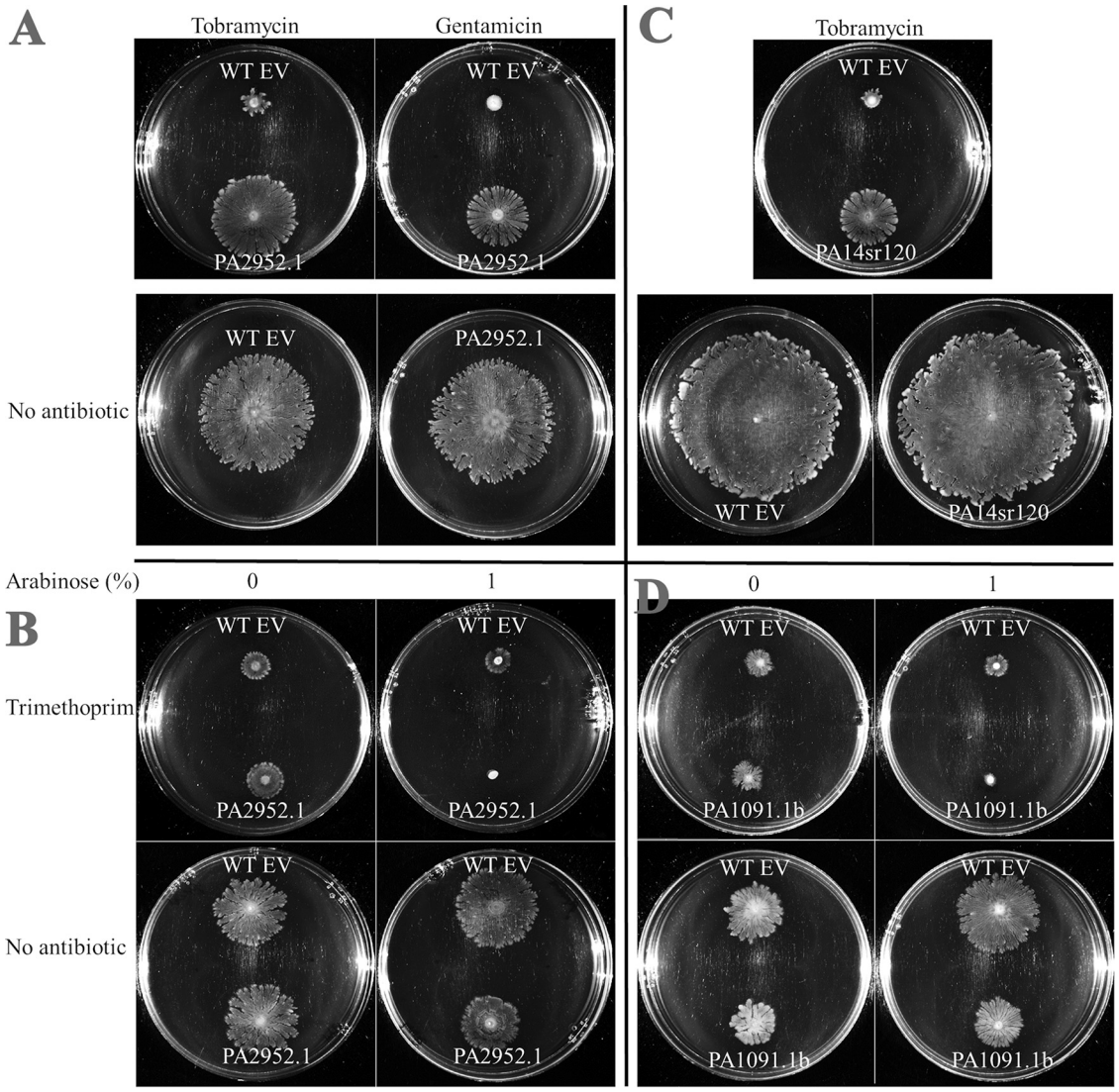

FIG 5 Antibiotic susceptibility phenotypes were affected by sRNAs under swarming conditions. (A) The strain overexpressing PA2952.1 showed resistance to tobramycin and gentamicin in BM2 glucose swarm plates with no arabinose, supplemented where indicated with 1 μg/ml antibiotic. $n = 3$. (B) Overexpression of PA2952.1 induced susceptibility to trimethoprim in BM2 glycerol swarm plates. Trimethoprim is included where indicated at 10 μg/ml. $n \geq 3$. (C) The PA14sr120 overexpression strain was resistant to tobramycin in BM2 glucose swarm plates with no arabinose. Tobramycin is included where indicated at 1 μg/ml. $n \geq 3$. (D) Overexpression of PA1091.1b increased susceptibility to trimethoprim in BM2 glycerol swarm plates. Trimethoprim is included where indicated at 10 μg/ml. $n \geq 3$.

Overexpression of PA2952.1 resulted in broad transcriptional changes, including the altered expression of 73 regulatory factors. The sRNA PA2952.1 was selected for study in greater detail due to its broad phenotypic effects and the lack of prior studies. To determine which genes or proteins caused the above-described phenotypic changes, RNA-Seq and proteomic analysis were performed on the WT strain overexpressing PA2952.1 compared to that with the EV control, by harvesting bacteria from the edges of swarming colonies grown with 1% arabinose. Substantial transcriptional changes were observed, encompassing 784 differentially expressed (DE) genes (absolute FC $>$ 1.5, adjusted P value $<$ 0.05; see Table S3 in the supplemental material). Of these, 339 genes were downregulated and 445 were upregulated. In proteomic studies, 18 proteins had decreased abundance and 41 were increased (absolute FC $>$ 1.25, $P < 0.05$; Table S3). An additional 386 proteins showed a significant absolute FC of $<$1.25. There were a large number (73 genes/proteins) of regulatory factors (transcriptional regulators, two-component systems, and sigma and anti-sigma factors) found

amongst these genes, which likely accounted for the large transcriptional changes observed (Table 1).

Two interesting regulatory factors with a protein absolute FC of >1.5 included DspI and ClpD. Relevant regulators in the RNA-Seq data with an absolute FC of >2 included *dksA2*, *pvdS*, *ptrC*, and *ppyR*. The importance of these regulators is described below.

Pilus and flagellar genes were downregulated in the PA2952.1 overexpression strain. Overexpression of PA2952.1 led to partial reductions in both swarming and swimming motilities (Fig. 2). Motility genes that were differentially expressed in the RNA-Seq and proteomics datasets are relevant for explaining this effect (Table 1). Certain pilus and flagellum-related genes and proteins were downregulated, including *chpC*, *fliE*, *pilA*, *pilGJ*, ChpA, PilC, PilU, PilW, PilY1, and PA1442 (Table 1 and Table S3), which could contribute to decreases in swarming and/or swimming motilities (8, 9). Other proteins or genes required for swarming (9) that were downregulated in the PA2952.1 overexpression strain were PA0591, PA0837 (*slyD*), PA0894, PA1827, PA2444 (*glyA2*), PA2630, PA3386, PA4005, PA4616, PA4775 (*greA*), PA5232, and PA5315 (*rpmG*); collectively, these may exert a multigenic influence to decrease swarming.

Genes in the *mexGHI-opmD* and *arn* operons were upregulated in the PA2952.1 overexpression strain. Related to the aminoglycoside resistance phenotype (Fig. 5A), the efflux proteins MexGH demonstrated a modest increase in the proteome (Table S3), while qRT-PCR also revealed a modest upregulation of these genes, particularly for *mexGH* (Table 2). The *mexGHI-opmD* efflux pump was previously shown to be involved in aminoglycoside efflux (31). The *mexF* transcript was also upregulated by 2.1-fold, as verified by qRT-PCR (see Table S4 in the supplemental material).

In addition, genes in the *arn* operon (*arnBCATF*) were upregulated (Table 1). These genes are involved in the aminoarabinosylation of lipopolysaccharide (LPS) to a more positively charged form, resulting in decreased self-promoted uptake across the outer membrane and in resistance to both aminoglycosides and cationic antimicrobial peptides (32). The *arn* operon is regulated by several different two-component systems; in this case, the sensor kinase *pmrB* was also upregulated (Table 1) (33).

Virulence and metal uptake pathways were dysregulated. Although significant differences were only observed for the cytotoxicity of the PA2952.1 overexpression strain in the absence of arabinose (Fig. 3A), numerous virulence factors were differentially expressed. In particular, two T3SS effectors, exotoxin ExoS and adenylate cyclase ExoY, as well as most T3SS genes, including the T3SS regulators *exsD* and *pcrH*, were downregulated in the arabinose-induced PA2952.1-overexpressing strain (Table 1 and Table S3), representing an explanation for why arabinose treatment suppressed the cytotoxicity defect. The altered expression of virulence factors, including *exoS*, *exoY*, *popB*, and *pcrD*, was verified by qRT-PCR (Table S3). Similarly, a repressor of T3SS, *ptrC*, was upregulated (Table 1) (34). Regarding other prominent virulence factors, genes and proteins in the T6SS were largely downregulated. Additionally, *pslN* and phenazine biosynthetic genes, except for *phzG1*, were upregulated, and three alginate biosynthetic genes were differentially expressed (Table 1 and Table S3). Interestingly, *algR*, *pvdS*, and *ppyR*, regulators of alginate, pyoverdine, and Psl biofilm matrix, were also upregulated (35–37). AlgR is also a global regulator that regulates twitching and swarming motility, pathogenesis, QS, and LPS and rhamnolipid production (36, 38–40).

Interestingly, genes and proteins involved in iron and zinc acquisition were upregulated, including *pvdS*, which is an iron-limitation sigma factor (41), and downstream pyoverdine biosynthetic genes, except for the *fdxA* and *iscA* regulators (Table 1). Regarding zinc acquisition, *dksA2*, a transcriptional regulator expressed selectively under zinc-limiting conditions (42), and *zur*, the zinc uptake regulator, were both upregulated, while the *cntIMLO* operon, involved in zinc uptake, was quite strongly upregulated (6.6- to 21.0-fold).

DISCUSSION

Here, we have probed the roles of sRNAs in motility and other adaptive processes. A total of 21 constructs were made featuring sRNAs that were differentially expressed

TABLE 1 Selected differentially expressed genes/proteins in the PA2952.1 overexpression strain compared by RNA-Seq and/or proteomics to the WT containing EV[a]

			RNA-Seq		Proteomics	
Locus tag	Gene name	Product name	FC	P_{adj}[b]	FC	*P*
Transcriptional regulators, two-component systems, and sigma factors						
PA0033	*hptC*	Histidine phosphotransfer protein	1.74	2.7E−03		
PA0048		Probable transcriptional regulator	−1.56	2.0E−02		
PA0155	*pcaR*	Transcriptional regulator	1.84	5.5E−14		
PA0175		Probable chemotaxis protein methyltransferase	1.57	5.8E−04		
PA0177		Probable purine-binding chemotaxis protein	1.52	1.7E−03		
PA0217		Probable transcriptional regulator	1.57	1.8E−03		
PA0403	*pyrR*	Transcriptional regulator	1.59	1.8E−04		
PA0459	*clpD*	Probable ClpA/B protease ATP binding subunit			1.51	1.7E−03
PA0463	*creB*	Two-component response regulator	1.81	2.4E−13		
PA0472	*fiuI*	Probable sigma-70 factor, extracytoplasmic function (ECF) subfamily	1.94	5.0E−05		
PA0528		Probable transcriptional regulator	1.78	1.9E−08		
PA0745	*dspI*	Dispersion inducer			2.19	2.2E−05
PA0828		Probable transcriptional regulator	−2.01	2.0E−02		
PA0877		Probable transcriptional regulator	−1.51	2.6E−02		
PA1179	*phoP*	Two-component response regulator	−1.51	6.1E−21		
PA1223		Probable transcriptional regulator	−1.56	3.7E−03		
PA1261	*lhpR*	Transcriptional regulator	1.96	2.3E−03		
PA1285		Probable transcriptional regulator	1.66	5.1E−07		
PA1290		Probable transcriptional regulator			1.30	1.1E−02
PA1328		Probable transcriptional regulator	1.65	5.1E−06		
PA1399		Probable transcriptional regulator	1.62	7.5E−03		
PA1431	*rsaL*	Regulatory protein	1.98	8.0E−08		
PA1627		Probable transcriptional regulator	2.21	1.4E−08		
PA1707	*pcrH*	Regulatory protein	−1.88	1.7E−04		
PA1714	*exsD*	Probable transcriptional regulator			−1.29	3.2E−02
PA1836		Probable transcriptional regulator	−1.51	2.5E−03		
PA1911	*femR*	Sigma factor regulator	1.93	1.5E−02		
PA1912	*femI*	ECF sigma factor	1.88	1.5E−03		
PA1930		Probable chemotaxis transducer	1.70	3.9E−04		
PA1980	*eraR*	Response regulator	−1.81	1.1E−02		
PA2126	*cgrC*	*cupA* gene regulator C	1.74	8.5E−05		
PA2126.1	*cgrB*	*cupA* gene regulator B	2.33	2.4E−07		
PA2337	*mtlR*	Transcriptional regulator	1.60	9.3E−04		
PA2426	*pvdS*	Sigma factor	2.07	2.0E−02		
PA2467	*foxR*	Anti-sigma factor	2.11	6.2E−07		
PA2486	*ptrC*	*Pseudomonas* type III repressor gene C	2.89	2.6E−13		
PA2511	*antR*	Probable transcriptional regulator	1.67	2.7E−03		
PA2663	*ppyR*	*psl* and pyoverdine operon regulator	2.14	1.5E−04		
PA2848		Probable transcriptional regulator	1.56	1.3E−02		
PA2870		Diguanylate cyclase	1.66	1.5E−06		
PA2882		Probable two-component sensor	2.31	5.0E−03		
PA2895	*sbrR*	Anti-sigma factor	1.52	2.2E−05		
PA2896	*sbrI*	Probable sigma-70 factor, ECF subfamily	1.50	1.6E−06		
PA2917		Probable transcriptional regulator	1.65	1.0E−06		
PA2931	*cifR*	Putative transcriptional regulator	−1.59	1.9E−03		
PA3161	*himD*	Integration host factor beta subunit	−2.17	2.0E−19	1.59	4.6E−02
PA3220		Probable transcriptional regulator	1.54	2.2E−04		
PA3458		Probable transcriptional regulator	−1.50	6.2E−03		
PA3757	*nagR*	Transcriptional regulator of *N*-acetylglucosamine catabolism operon	1.52	2.6E−03		
PA3878	*narX*	Two-component sensor	1.57	1.1E−07		
PA3899	*fecI*	Probable sigma-70 factor, ECF subfamily	1.62	7.4E−03		
PA4057	*nrdR*	Transcriptional repressor	−1.54	2.6E−06		
PA4070		Probable transcriptional regulator	1.98	1.1E−05		
PA4108		Cyclic di-GMP phosphodiesterase	1.58	1.8E−06		
PA4280	*birA*	Bifunctional protein	−1.53	2.1E−05		
PA4596	*esrC*	Envelope-stress regulated repressor	1.69	8.3E−04		

(Continued on next page)

TABLE 1 (Continued)

Locus tag	Gene name	Product name	RNA-Seq FC	RNA-Seq P_{adj}[b]	Proteomics FC	Proteomics *P*
PA4726	*cbrB*	Two-component response regulator	1.51	4.4E−25		
PA4777	*pmrB*	Two-component regulator system signal sensor kinase	1.54	5.4E−03		
PA4781		Cyclic di-GMP phosphodiesterase	1.58	5.4E−06		
PA4784		Probable transcriptional regulator	1.53	2.0E−05		
PA4844	*ctpL*	Chemotactic sensor	3.97	1.8E−11		
PA4857	*tspR*	Transcriptional regulator	1.93	7.0E−05		
PA4914	*amaR*	Transcriptional regulator	1.62	1.5E−05		
PA5029		Probable transcriptional regulator	1.54	2.5E−05		
PA5060	*phaF*	Polyhydroxyalkanoate synthesis protein PhaF			1.82	2.6E−03
PA5124	*ntrB*	Two-component sensor	1.72	6.6E−06		
PA5189		Probable transcriptional regulator	1.59	3.6E−05		
PA5261	*algR*	Alginate biosynthesis regulatory protein	1.58	5.2E−08		
PA5288	*glnK*	Nitrogen regulatory protein P-II 2	1.58	4.5E−04		
PA5356	*glcC*	Transcriptional regulator	2.19	1.1E−18		
PA5536	*dksA2*	Transcriptional regulator	27.7	4.2E−06		
PA5403		Probable transcriptional regulator	1.70	1.1E−03		
PA5499	*zur*	Zinc uptake regulator	2.27	6.3E−06		
Motility and related genes						
PA0408	*pilG*	Twitching motility protein			−1.33	4.9E−02
PA0411	*pilJ*	Twitching motility protein			−1.32	1.6E−04
PA0415	*chpC*	Probable chemotaxis protein	−1.56	3.3E−06		
PA1100	*fliE*	Flagellar hook-basal body complex protein	−1.55	1.6E−06		
PA1442		Conserved hypothetical protein	−1.52	1.0E−09		
PA4525	*pilA*	Type 4 fimbrial precursor	−2.86	7.2E−24		
PA5043	*pilN*	Type 4 fimbrial biogenesis protein			1.38	9.1E−03
Multidrug efflux and LPS[c] modification						
PA2494	*mexF*	Resistance-nodulation-cell division (RND) multidrug efflux transporter	1.66	2.7E−02		
PA2525	*opmB*	Outer membrane efflux protein			1.67	3.0E−02
PA3522	*mexQ*	Efflux pump membrane transporter	−1.63	1.8E−02		
PA4374	*mexV*	RND multidrug efflux membrane fusion protein	2.89	2.2E−18	1.11	2.8E−02
PA3552	*arnB*	UDP-4-amino-4-deoxy-L-arabinose-oxoglutarate aminotransferase	2.06	1.8E−04		
PA3553	*arnC*	Undecaprenyl-phosphate 4-deoxy-4-formamido-L-arabinose transferase	2.48	3.1E−08		
PA3554	*arnA*	Bifunctional polymyxin resistance protein	1.61	9.4E−03		
PA3556	*arnT*	Inner membrane L-Ara4N transferase	1.71	1.5E−03		
PA3558	*arnF*	Probable 4-amino-4-deoxy-L-arabinose-phosphoundecaprenol flippase subunit	2.45	1.0E−05		
PA3559		Probable nucleotide sugar dehydrogenase	1.97	3.8E−04		
DNA synthesis and cell division						
PA0010	*tag*	DNA-3-methyladenine glycosidase I	−1.66	1.1E−06		
PA0441	*dht*	Dihydropyrimidinase	2.10	1.9E−02		
PA0582	*folB*	Dihydroneopterin aldolase	−2.32	5.3E−13		
PA0733		Probable pseudouridylate synthase	3.68	5.8E−21		
PA0807	*ampDh3*	Peptidoglycan catabolic process	2.34	1.5E−11		
PA0973	*oprL*	Peptidoglycan-associated lipoprotein precursor	−1.54	1.5E−07		
PA1279	*cobU*	nicotinate-nucleotide-dimethylbenzimidazole phosphoribosyltransferase	−1.53	3.0E−03		
PA1524	*xdhA*	Xanthine dehydrogenase	1.63	2.0E−05		
PA1678		Probable DNA methylase	−1.60	7.1E−06		
PA1920	*nrdD*	Class III (anaerobic) ribonucleoside-triphosphate reductase subunit	1.72	1.0E−02		
PA3245	*minE*	Cell division topological specificity factor	−1.73	3.9E−20		
PA3807	*ndk*	Nucleoside diphosphate kinase	−1.55	6.3E−09		
PA4042	*xseB*	Exodeoxyribonuclease VII small subunit	−2.10	2.7E−08		
PA4172		Probable nuclease	2.42	3.7E−10		
PA4238	*rpoA*	DNA-directed RNA polymerase alpha chain	−1.68	1.1E−09		

(Continued on next page)

TABLE 1 (Continued)

Locus tag	Gene name	Product name	RNA-Seq FC	RNA-Seq P_{adj} [b]	Proteomics FC	Proteomics *P*
PA4269	*rpoC*	DNA-directed RNA polymerase beta chain	−1.63	6.0E−11		
PA4270	*rpoB*	DNA-directed RNA polymerase beta chain	−1.55	1.5E−10		
PA4275	*nusG*	Transcription antitermination protein	−2.11	4.0E−19		
PA5538	*amiA*	*N*-acetylmuramoyl-L-alanine amidase	4.63	4.7E−04		
PA5541	*pyrQ*	Dihydroorotase	6.74	7.7E−04		
Virulence factors						
PA0081	*fha1*	Type VI secretion protein	1.51	9.1E−11		
PA0082	*tssA1*	Type VI secretion protein			1.39	6.8E−03
PA0090	*clpV1*	Type VI secretion protein	−1.51	7.3E−04		
PA1512	*hcpA*	Secreted protein	1.60	1.4E−02		
PA1664	*orfX*	Type VI secretion protein	−2.32	6.1E−03		
PA1666	*lip2*	Type VI secretion protein	−1.77	2.5E−05		
PA1670	*stp1*	Type VI secretion protein	−1.56	5.0E−03		
PA1694	*pscQ*	Translocation protein in type III secretion	−2.28	1.2E−03		
PA1700	*pcr2*	Type III secretion chaperone	−3.32	9.0E−03		
PA1703	*pcrD*	Type III secretory apparatus protein	−1.59	2.0E−06		
PA1706	*pcrV*	Type III secretion protein	−1.61	9.4E−04		
PA1708	*popB*	Translocator protein	−2.16	8.9E−11		
PA1709	*popD*	Translocator outer membrane protein precursor	−1.79	1.5E−06		
PA1710	*exsC*	Exoenzyme S synthesis protein C precursor	−1.73	2.4E−08		
PA1712	*exsB*	Exoenzyme S synthesis protein B	−1.76	3.1E−10		
PA1715	*pscB*	Type III export apparatus protein	−2.41	3.2E−04		
PA1717	*pscD*	Type III export protein	−2.22	9.0E−05		
PA1719	*pscF*	Type III export protein	−1.59	3.0E−03		
PA1720	*pscG*	Type III export protein	−1.71	6.4E−03		
PA1722	*pscI*	Type III export protein	−2.15	3.5E−04		
PA1723	*pscJ*	Type III export protein	−1.74	4.1E−06		
PA2191	*exoY*	Adenylate cyclase	−2.04	6.6E−07		
PA2244	*pslN*	Hypothetical protein	1.68	8.8E−03		
PA2368	*hsiF3*	Type VI secretion protein	−1.64	2.3E−03		
PA3291	*tli1*	Type VI secretion protein	−1.66	7.0E−04		
PA3841	*exoS*	Exoenzyme S	−1.53	5.3E−06		
Iron and zinc uptake						
PA0470	*fiuA*	Ferrichrome receptor	4.33	2.3E−23		
PA0781		Putative TonB-dependent receptor	14.6	3.2E−08		
PA1922		Putative TonB-dependent receptor	8.39	2.6E−04		
PA2393		Putative dipeptidase	1.71	2.9E−02		
PA2397	*pvdE*	Pyoverdine biosynthesis protein	2.61	6.6E−04		
PA2411		Probable thioesterase	1.55	1.3E−02		
PA2413	*pvdH*	L-2,4-diaminobutyrate:2-ketoglutarate 4-aminotransferase	1.56	1.4E−02		
PA3621	*fdxA*	Ferredoxin I	−2.13	3.1E−09		
PA3812	*iscA*	Probable iron-binding protein	−1.56	1.0E−08		
PA4229	*pchC*	Pyochelin biosynthetic protein	1.68	8.9E−07		
PA4358	*feoB*	Ferrous iron transport protein B	1.59	1.8E−02		
PA4655	*hemH*	Ferrochelatase	1.57	8.1E−12		
PA4834	*cntI*	EamA-like transporter family	6.59	3.8E−03		
PA4835	*cntM*	Opine metallophore dehydrogenase	9.37	1.9E−04		
PA4836	*cntL*	Nicotianamine synthase	11.4	4.6E−05		
PA4837	*cntO*	TonB-dependent siderophore receptor	21.0	1.6E−07		
PA4880		Probable bacterioferritin	2.72	1.1E−10		
PA5500	*znuC*	Zinc transport protein	2.34	9.5E−08		

[a]Cutoffs used were a *P* value of ≤0.05, an absolute fold change (FC) of ≥1.5 for transcriptome sequencing (RNA-Seq), and an absolute FC of ≥1.25 for proteomics, although proteins with an absolute FC of <1.25 are also shown if there was a corresponding RNA-Seq or quantitative reverse transcriptase PCR (qRT-PCR) value. $n \geq 3$. WT, wild type; EV, empty cloning vector.
[b]P_{adj}, adjusted *P* value.
[c]LPS, lipopolysaccharide.

TABLE 2 Upregulation of genes in the PA2952.1 overexpression strain relative to the WT containing EV[a]

Gene	Fold change	*P*
mexG	1.7 ± 0.2	1.0E−02
mexH	1.7 ± 0.2	2.3E−02
mexI	1.8 ± 0.3	6.4E−02
opmD	1.8 ± 0.5	1.5E−01

[a]Genes in the *mexGHI-opmD* operon were modestly upregulated in the PA2952.1 overexpression strain compared by qRT-PCR to the WT containing EV. Bacteria were harvested from BM2 glycerol swarm plates with 1% arabinose and 0.1% Casamino acids. Mean ± standard error is shown for $n = 3$, and *P* values were determined by unpaired *t* test.

during swarming motility, and functions were identified for five of these (including PA0805.1) when cloned to enable overexpression, since this enhances the known inhibitory functions of sRNAs. In contrast, in this study, no phenotypes were observed for the overexpression of RsmY. This may be due to an insufficiency of RsmA, the cognate RNA-binding protein involved in RsmY-mediated regulation, or to a redundancy with sRNA RsmZ; for example, when RsmY was overexpressed, RsmZ could have been downregulated to cancel out any effects (24). We also did not observe any phenotype for SrbA, but this might have been because the sRNA was overexpressed rather than deleted. Furthermore, it is worth noting that the original study did not observe any phenotypic effects in a WT strain natively or ectopically expressing SrbA (23).

Two of the sRNAs for which we demonstrated functions in overexpression strains, namely PrrH and PA2952.1, showed evidence of cross-regulation (see Table S1 in the supplemental material) and are linked to iron metabolism. Fur, the ferric uptake regulator, is a transcriptional repressor of PrrH under iron-replete conditions, although it can also function as an activator (16, 26). Under iron-depleted conditions, the expression of PrrH is highly induced (26), while it is upregulated by 163-fold under swarming conditions (22). Results presented here indicated that PrrH was involved in suppressing cytotoxicity (Fig. 3B) and in the production of pyoverdine (Fig. 4) and that overexpression of PrrH led to a reduction in swimming motility (Fig. 2). Fur also controls expression of the iron starvation sigma factor PvdS, which controls downstream expression of the siderophore pyoverdine (41). In the PA2952.1 overexpression strain, *pvdS* was upregulated, as were pyoverdine-mediated iron acquisition genes, while T3SS toxins were downregulated, and swimming motility was decreased to a similar extent as for the PrrH overexpression strain (Table 1 and Fig. 2).

Iron metabolism is often interrelated with virulence factors, and here, the *ptrC* transcript, encoding a repressor of the T3SS, was upregulated 2.9-fold in the RNA-Seq data (Table 1). This could contribute to the downregulation of T3SS genes observed in Table 1. Decreases in both T3SS and swarming motility are consistent with a study that found a positive association between T3SS and swarming in clinical isolates (43).

Regarding phenotypes observed under swarming conditions, genes and proteins involved in DNA synthesis, including those involved in pyrimidine metabolism, were differentially expressed (Table 1). This could contribute to the increased susceptibility to trimethoprim observed in the PA2952.1 overexpression strain (Fig. 5B), since trimethoprim inhibits the enzyme dihydrofolate reductase, causing a decrease in the levels of tetrahydrofolate, which is required for thymidylate production (44). Furthermore, subinhibitory trimethoprim has been shown to impact on cell division (45).

Regulatory proteins that may be important in regulating the motile-sessile switch include DspI, which increased in abundance by more than twofold in the PA2952.1 overexpression strain compared to that in the WT EV (Table 1). DspI is a putative enoyl-coenzyme A hydratase that produces an autoinducer, *cis*-2-decenoic acid (46). This autoinducer is a fatty acid involved in intercellular communication that induces biofilm dispersion in *P. aeruginosa* (46) and is thus an interesting regulatory factor that may be involved in regulating the motile-sessile switch. Mutant studies showed that DspI is also important for flagellar assembly, swarming motility, virulence in murine and *C.*

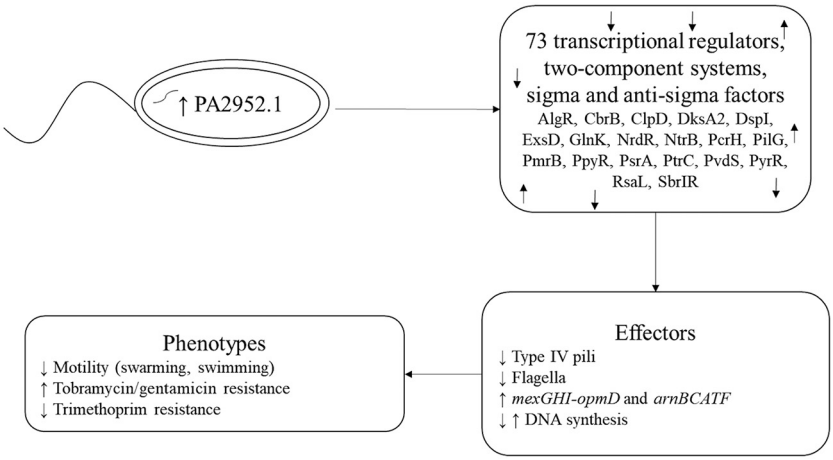

FIG 6 Proposed model for how the overexpression of PA2952.1 causes the differential expression of many genes, resulting in altered phenotypes. Connecting arrows represent direct or indirect regulation.

elegans infection models, and the production of pyoverdine (47, 48). Other proteins that likely form part of an operon with DspI (PA0744, PA0746, and PA0747) were also increased in the proteome (see Table S3 in the supplemental material).

Another protein that may be involved in motile-sessile switching and biofilm dispersion is the protease ClpD, which increased in abundance by 1.5-fold compared to that in the WT EV strain (Table 1). ClpD functions as a chaperone for the cleavage of the chemotactic transducer BdlA and is required for virulence in a rat lung infection model (49, 50). The cleaved BdlA product was in turn required for biofilm dispersal (49).

Proteomic and transcriptomic data often do not correlate well due to a number of reasons. Not only are these two different approaches that rely on different detection methods, but due to posttranscriptional modification and widely different half-lives (mRNA has a half-life of only 40 to 60 s), the proteome is expected to be distinct from the transcriptome. Thus, studies have shown that the correlation between proteomics and RNA-Seq is often quite low (51, 52). Nevertheless, a closer analysis of the data without an FC cutoff revealed a reasonable correlation between 91 genes and proteins, as shown in Fig. S7 in the supplemental material.

Three *in silico* sRNA target prediction tools, IntaRNA2, RNAPredator, and TargetRNA2, were used to predict sRNA targets for PA2952.1 based on hybridization near the 5′ end of mRNA (see Table S5 in the supplemental material). Although one of the predictions was an uncharacterized transcriptional regulator (PA0828), the results were not particularly compelling as an explanation for the many transcriptomic and phenotypic differences observed for the PA2952.1 overexpression strain. Consistent with this, a recent paper found that none of the available tools shows high reliability (53), possibly because the required level of homology between sRNAs and their targets is strongly mitigated by RNA binding proteins.

Upon overexpression of the sRNA PA2952.1, 784 genes showed significant changes in abundance (Table S3), accompanied by several phenotypic differences (Fig. 2 and Fig. 5A and B), indicating that this has the hallmarks of a global regulatory system. Based on this study, we propose a model to account for the surprisingly large amount of differential expression (Fig. 6). In a hierarchical fashion, overexpression of PA2952.1 directly or indirectly led to alterations in the levels of 73 regulatory factors, which then in turn influenced the expression of downstream genes. For example, AlgR, which was affected by PA2952.1, could in turn influence alginate synthesis genes; ExsD, PcrH, and PtrC are all able to influence the T3SS; PvdS and PpyR could influence iron uptake genes and Psl matrix biosynthesis; PilG could influence type IV pilus expression; and PmrB could influence the expression of the *arn* operon. Such hierarchical regulation

might also involve additional downstream genes without a known regulator, or genes with multiple potential regulators, and further detailed experimentation would be required to determine the exact pathway through which PA2952.1 was acting. The regulatory proteins DspI and ClpD (and likely others) may also be involved in controlling the motile-sessile switch. Downregulation of pilus and certain flagellar genes, as well as of genes required for swarming, would lead to decreases in swarming and swimming motilities, upregulation of the *mexGHI-opmD* and *arn* operons likely mediates aminoglycoside resistance, and the differential expression of certain genes involved in DNA synthesis could influence trimethoprim susceptibility. Overall, this highlights a potential key role for the sRNA PA2952.1 in modulating the expression of many proteins at both the transcriptional and posttranscriptional levels, thereby controlling bacterial lifestyles, and demonstrates that predictive programs that usually indicate a very modest number of target genes have the potential to dramatically underestimate the number of actual targets, and more importantly, the broad overall impact of sRNAs.

MATERIALS AND METHODS

Bacterial strains and growth conditions. *P. aeruginosa* strain PAO1 H103 and the Δ*prrH* deletion mutant (26) were routinely grown in Luria-Bertani (LB) broth and BM2 minimal medium (62 mM potassium phosphate buffer [pH 7], 0.5 mM $MgSO_4$, 10 μM $FeSO_4$, and carbon and nitrogen sources as indicated). LB overnight cultures were diluted 1/50 and grown to the mid-log phase (optical density at 600 nm [OD_{600}] of 0.3 to 0.6) to initiate motility studies. A list of strains used in this study is included in Table S6 in the supplemental material.

Construction of overexpression plasmids. PAO1 WT genomic DNA was isolated as specified in the Qiagen DNeasy blood and tissue kit protocol. DNA (300 ng) was amplified by PCR, using the primers described in Table 3. PCR products were then cloned using one of two cloning strategies, as described in Table S7 in the supplemental material. PCR products that were cloned via the TOPO strategy were gel extracted with the GeneJet gel extraction kit (Thermo Fisher) and TOPO cloned (Invitrogen). TOPO reaction mixtures were transformed into TOP10 *Escherichia coli* cells, and transformants were selected with 50 μg/ml kanamycin (TOPO). Plasmids were subsequently isolated as specified in the Thermo Fisher kit and digested with the restriction endonucleases indicated in Table S7. This allowed the sRNAs to be cloned in two different orientations, termed a and b. After the fragments were gel extracted, they were ligated into the similarly digested vector pHERD20T with T4 DNA ligase (Thermo Scientific), transformed into TOP10 *E. coli* cells, and transformants were selected with 100 μg/ml ampicillin. PCR products that were cloned via the direct strategy were PCR purified using a PCR purification kit (Thermo), and then digested with the restriction enzymes indicated in Table S7. Next, digested fragments were gel extracted and ligated as described above and then transformed into TOP10 *E. coli* cells, and transformants were selected with 100 μg/ml ampicillin. Plasmid sequences were confirmed by Sanger sequencing at the Sequencing and Bioinformatics Consortium at UBC.

Transformation of *P. aeruginosa*. Electrocompetent *P. aeruginosa* cells were transformed with either pHERD20T (empty cloning vector [EV]) or pHERD20T containing various inserts, according to Choi et al. (54). The wild-type (WT) was transformed with the EV pHERD20T and all of the sRNA overexpression vectors. The Δ*prrH* mutant was transformed with both EV and PrrH-pHERD20T. Transformants were selected with 300 μg/ml carbenicillin. Overexpression from the vector was induced by adding arabinose at the indicated concentrations. This method has been demonstrated previously to generate reliable and stable overexpression under experimental conditions (28).

Motility assays. The concentration of agar and nitrogen source used in BM2 was varied to allow for different kinds of motility. Glucose was often replaced with an alternative carbon source (as indicated), as glucose represses expression from the P_{BAD} promoter of the plasmid pHERD20T (55). Swimming motility was assayed using 0.25% agar (wt/vol) with 7 mM $(NH_4)_2SO_4$ as the nitrogen source and 20 mM potassium succinate (pH 7.0) as the carbon source, unless otherwise indicated. For swarming assays, plates were solidified with 0.5% agar (wt/vol); 0.1% Casamino acids was used as the nitrogen source and 0.4% glycerol (wt/vol) as the carbon source, unless otherwise indicated. Swimming and swarming BM2 plates were composed of 25 ml medium per plate and dried for 1 h. In contrast, LB medium was used for twitching motility, with 1% agar and 10 ml medium per plate, and plates were dried overnight. Arabinose was included where indicated for plasmid induction. All plates were stab (swim and twitch) or spot (swarm) inoculated with 1.5 μl of mid-log-phase bacteria. After inoculation, plates were incubated for 16 to 20 h at 37°C and imaged on the ChemiDoc touch imaging system (Biorad).

Growth curves. Growth curves were performed as previously described (28) in either liquid BM2 swarming medium (with 0.4% glycerol [wt/vol], 0.1% Casamino acids [wt/vol], and 1% arabinose [wt/vol]) or DMEM (no glucose, 1% fetal bovine serum [FBS], 1% sodium pyruvate, and 1% arabinose).

RNA-Seq and proteomics. Bacteria were grown and harvested simultaneously for RNA-Seq and proteomic analysis as previously described by harvesting from the leading edge of the swarm, or the first ~1 to 2 mm (28). RNA isolation, library preparation, and data analysis were performed as previously described and with five biological replicates (28). Protein digestion and quantification, tandem mass tag (TMT) labeling, mass spectrometry, and differential analysis of proteins were performed as previously described (28). For TMT labeling, four TMT10 channels (TMT0 to TMT3) were assigned to samples from

TABLE 3 Primers used in this study

Name	Purpose	Sequence (5′→3′)
exoS F	qPCR	GCCGTCGTGTTCAAGCAGAT
exoS R	qPCR	AGTCCTTCCGGTGTCAGGGT
exoY F	qPCR	GTGGCCAGGCAGACGAATAC
exoY R	qPCR	TTCACCGAGAAGCCCTTGG
mexF F	qPCR	AACGCCATCCGCGAGCAGAACC
mexF R	qPCR	GACAGCGCGTTGAGCGAGAAGC
mexG F	qPCR	ACTCGCTCGAAAGCAACTGG
mexG R	qPCR	AGGCTGGCCTGATAGTCGAA
mexH F	qPCR	ATCCGTCTCAAGGCGCAGTT
mexH R	qPCR	TTGTCCAGCTGTTCCTGCGA
mexI F	qPCR	ATCACCGTCACCACCGAGTA
mexI R	qPCR	AAAGGTAGTCGATGCCCTCC
opmD F	qPCR	TACAGCCGCAGCATCGAACA
opmD R	qPCR	CCGAACAGGTCGATTTCCCA
pcrD F	qPCR	GAAGGAGAAGGACGTGGTGC
pcrD R	qPCR	GCAGATAGGCGGGAAGGATAT
popB F	qPCR	CGCCTGAAGGAAGAGCTGAG
popB R	qPCR	AGGTGTGCAGGGTTTCACC
prrF1 F	qPCR	TCGCGAGATCAGCCGG
prrF1 R	qPCR	GCCTGATGAGGAGATAATCTGAAGA
psrA F	qPCR	GGAAAAGGAGCTGGATCGTC
psrA R	qPCR	AGCGCATGAAGATCGACAG
rpoD F	qPCR	TCACGCACGCAGAGTTGCAT
rpoD R	qPCR	AAGCTGGTGCCCAAGCAGTT
PA0730.1 F	Cloning	GACTCTAGACGATGGGAACGCGGCGA
PA0730.1 R	Cloning	CTCGGTACCGTCCCTTTCCTTCCCGGCAT
PA0805.1 F	Cloning	GACTCTAGAATGGAGCAGCGTATATTGC
PA0805.1 R	Cloning	CTCGGTACCCTGCGTACCAAACTGAAAGTC
PA0958.1 F	Cloning	GACTCTAGACTTGGCGATAGTTGAGGTTCC
PA0958.1 R	Cloning	CTCGGTACCGTTTGCTTTCAAACAGAATAGCCT
PA1091.1 F	Cloning	CTCGGTACCAACTTCCACCCTCTGCCG
PA1091.1 R	Cloning	GACTCTAGAGGTGATTTCCTCCAAAGGACC
PA14sr120 F	Cloning	CTCGGTACCATGGAGCAGCGTATATTGC
PA14sr120 R	Cloning	GACTCTAGATAGTACCTGAACTGCCAGC
PA2461.1 F	Cloning	GACTCTAGATCTTCAGCTCAGACACAGGTT
PA2461.1 R	Cloning	CTCGGTACCCTTAGAGGAAGGTCCATTCAAACA
PA2461.3 F	Cloning	GACTCTAGACTGTACCGCGAGCCCC
PA2461.3 R	Cloning	CTCGGTACCCAACGCTGGAGTATCATCCACT
PA2952.1 F	Cloning	CTCGGTACCGCCCGTATCTTGACCGGAT
PA2952.1 R	Cloning	GACTCTAGATAGCTGCATGGGCAGGTC
PA2952.1W F	Cloning	CTCGGTACCATAAGGATGTCGCCAGACAGG
PA2952.1W R	Cloning	GACTCTAGAGAGCGGGCGCATTAT
PA3159.1 F	Cloning	CTCGGTACCCACCCCGCGATTGCC
PA3159.1 R	Cloning	GACTCTAGATAGTTATTGAAGTGGTGATGCGT
PA4539.1 F	Cloning	GACTCTAGAGCCGCCAGACCGAACG
PA4539.1 R	Cloning	CTCGGTACCGCGGAAAAGCTGGATGCATGG
PA4656.1 F	Cloning	CTCGGTACCATTCCGGCGTTATCCTGTGA
PA4656.1 R	Cloning	GACTCTAGACCTCTCTGGTTGTGTAGCGT
PA5078.1 F	Cloning	GACTCTAGACGTCCGTGAACATGAATTACT
PA5078.1 R	Cloning	CTCGGTACCCTGTACAGGACAGGCCG
PA5304.1 F	Cloning	GACTCTAGACAGTATAGGAAGAGGCAGGCA
PA5304.1 R	Cloning	CTCGGTACCAGGCTCCGCGAGCGCTCTGG
PrrH F	Cloning	GGATCCAACTGGTCGCGAGAT
PrrH R	Cloning	TCTAGAAGGAAGGGCGCGAGG
RsmY F	Cloning	CTCGGTACCGTCAGGACATTGCGCAGGAA
RsmY R	Cloning	GACTCTAGAAAAACCCCGCCTTTTGGGC
SrbA F	Cloning	CTCGGTACCATCAGGGGCTCTGAAACGAC
SrbA R	Cloning	GACTCTAGATCAAGAAATGTATTGGTTGAGCACC

the WT EV strain, and three TMT10 channels (TMT4 to TMT6) to samples from the PA2952.1 strain. This represented four biological replicates for the WT EV strain and three replicates for the PA2952.1 strain.

Quantitative reverse transcriptase polymerase chain reaction. Swarming BM2 plates containing 0.1% Casamino acids (wt/vol), 0.4% glycerol, and 0% or 1% arabinose (as indicated) were grown overnight at 37°C. RNA was isolated, DNase digested, and assayed by qRT-PCR as previously described (28). Quantification cycle (C_q) values were normalized to the housekeeping gene *rpoD* using the threshold cycle ($\Delta\Delta C_T$) method. Primers used for quantitative PCR (qPCR) are described in Table 3.

Tobramycin kill curve. Tobramycin kill curves were performed as described previously (12) with minor modifications. Briefly, bacteria were harvested from BM2 glucose swarm (0.5% agar) and swim (0.3% agar) plates in 62 mM potassium phosphate buffer (pH 7.0), and treated with 20 μg/ml tobramycin in a 5-ml volume with aeration at room temperature.

MIC assay. MICs were determined as previously described (28) in BM2 with 0.4% glycerol (wt/vol) and 0.1% Casamino acids (wt/vol), no $(NH_4)_2SO_4$, and arabinose as indicated.

Adherence assay. Overnight cultures were diluted to a final OD_{600} of 0.03 in 90% LB supplemented with 5% arabinose (wt/vol) and seeded at 100 μl/well in 96-well flat-bottomed polystyrene plates. After incubation for 4 h at 37°C, unattached cells were removed by discarding the medium and rinsing three times with distilled water (dH_2O). Crystal violet (105 μl; 0.1%) was added and incubated with shaking for 20 minutes at room temperature, and then the plates were rinsed three times with dH_2O and the crystal violet was solubilized by adding 110 μl 70% (vol/vol) ethanol and shaking for 20 minutes at room temperature. Then, the absorbance at 595 nm was read in an Epoch plate reader (BioTek).

Pyoverdine assay. Bacteria were grown overnight in Casamino acid medium (0.5% Casamino acids, 0.1 mM $MgSO_4$, and 7 mM potassium phosphate buffer [pH 7.0]). Turbid cultures were pelleted, and the supernatants were collected in fresh tubes. Next, 5 μl of supernatant was mixed with 995 μl 10 mM Tris (pH 6.8). Then, the fluorescence was monitored on a PerkinElmer 168 LS 55 fluorescence spectrometer with an excitation wavelength of 405 nm, by scanning the emission spectrum from 400 to 700 nm.

Cytotoxicity against HBE cells. Cytotoxicity against human bronchial epithelial 16HBE14o$^-$ (HBE) cells was assessed by the lactate dehydrogenase (LDH) assay as previously described (28).

***In silico* sRNA target prediction.** sRNA targets were predicted as previously described (28) using three tools, IntaRNA2 (56), RNAPredator (57), and TargetRNA2 (58).

Data availability. RNA-Seq data were deposited in the GEO database under accession number GSE146765. Proteomics data were deposited in MassIVE under index number MSV000085955.

SUPPLEMENTAL MATERIAL

Supplemental material is available online only.

SUPPLEMENTAL FILE 1, PDF file, 0.8 MB.

SUPPLEMENTAL FILE 2, XLSX file, 0.2 MB.

ACKNOWLEDGMENTS

Research reported in this publication was supported by a grant from the Canadian Institutes for Health Research (FDN-154287). S.R.C. was the recipient of CIHR Frederick Banting and Charles Best Canada Graduate Scholarship Master's (CGS-M) and Doctoral Awards (CGS-D) and of a four-year fellowship for PhD students from the University of British Columbia (UBC). R.E.W.H. holds a Canada Research Chair in Health and Genomics and a UBC Killam Professorship.

The content is solely the responsibility of the authors and does not necessarily represent the official views of the Canadian Institutes for Health Research.

We thank lab members for insightful advice, particularly Amy Lee for coordinating the multiple omics projects and Reza Falsafi for RNA-Seq sample preparation.

REFERENCES

1. Chiriac A, Brzezinski P, Foia L, Marincu I. 2014. Chloronychia: green nail syndrome caused by *Pseudomonas aeruginosa* in elderly persons. Clin Interv Aging 10:265–267.
2. Davies JC. 2002. *Pseudomonas aeruginosa* in cystic fibrosis: pathogenesis and persistence. Paediatr Respir Rev 3:128–134. https://doi.org/10.1016/S1526-0550(02)00003-3.
3. Mittal R, Aggarwal S, Sharma S, Chhibber S, Harjai K. 2009. Urinary tract infections caused by *Pseudomonas aeruginosa*: a minireview. J Infect Public Health 2:101–111. https://doi.org/10.1016/j.jiph.2009.08.003.
4. Moore NM, Flaws ML. 2011. Introduction: *Pseudomonas aeruginosa*. Clin Lab Sci 24:41–42. https://doi.org/10.29074/ascls.24.1.41.
5. Fernández L, Hancock REW. 2012. Adaptive and mutational resistance: role of porins and efflux pumps in drug resistance. Clin Microbiol Rev 25:661–681. https://doi.org/10.1128/CMR.00043-12.
6. Jo JTH, Brinkman FSL, Hancock REW. 2003. Aminoglycoside efflux in *Pseudomonas aeruginosa*: involvement of novel outer membrane proteins. Antimicrob Agents Chemother 47:1101–1111. https://doi.org/10.1128/AAC.47.3.1101-1111.2003.
7. Yeung ATY, Parayno A, Hancock REW. 2012. Mucin promotes rapid surface motility in *Pseudomonas aeruginosa*. mBio 3:e00073-12. https://doi.org/10.1128/mBio.00073-12.
8. Köhler T, Curty LK, Barja F, van Delden C, Pechère J-C. 2000. Swarming of

Pseudomonas aeruginosa is dependent on cell-to-cell signaling and requires flagella and pili. J Bacteriol 182:5990–5996. https://doi.org/10.1128/JB.182.21.5990-5996.2000.
9. Yeung ATY, Torfs ECW, Jamshidi F, Bains M, Wiegand I, Hancock REW, Overhage J. 2009. Swarming of *Pseudomonas aeruginosa* is controlled by a broad spectrum of transcriptional regulators, including MetR. J Bacteriol 191:5592–5602. https://doi.org/10.1128/JB.00157-09.
10. Overhage J, Bains M, Brazas MD, Hancock REW. 2008. Swarming of *Pseudomonas aeruginosa* is a complex adaptation leading to increased production of virulence factors and antibiotic resistance. J Bacteriol 190:2671–2679. https://doi.org/10.1128/JB.01659-07.
11. Lai S, Tremblay J, Déziel E. 2009. Swarming motility: a multicellular behaviour conferring antimicrobial resistance. Environ Microbiol 11:126–136. https://doi.org/10.1111/j.1462-2920.2008.01747.x.
12. Coleman SR, Blimkie T, Falsafi R, Hancock REW. 2020. Multidrug adaptive resistance of *Pseudomonas aeruginosa* swarming cells. Antimicrob Agents Chemother 64:e01999-19. https://doi.org/10.1128/AAC.01999-19.
13. Gómez-Lozano M, Marvig RL, Molin S, Long KS. 2012. Genome-wide identification of novel small RNAs in *Pseudomonas aeruginosa*. Environ Microbiol 14:2006–2016. https://doi.org/10.1111/j.1462-2920.2012.02759.x.
14. Wurtzel O, Yoder-Himes DR, Han K, Dandekar AA, Edelheit S, Greenberg EP, Sorek R, Lory S. 2012. The single-nucleotide resolution transcriptome of *Pseudomonas aeruginosa* grown in body temperature. PLoS Pathog 8:e1002945. https://doi.org/10.1371/journal.ppat.1002945.
15. Kavita K, de Mets F, Gottesman S. 2018. New aspects of RNA-based regulation by Hfq and its partner sRNAs. Curr Opin Microbiol 42:53–61. https://doi.org/10.1016/j.mib.2017.10.014.
16. Pita T, Feliciano JR, Leitão JH. 2018. Small noncoding regulatory RNAs from *Pseudomonas aeruginosa* and *Burkholderia cepacia* complex. Int J Mol Sci 19:3759. https://doi.org/10.3390/ijms19123759.
17. Prévost K, Desnoyers G, Jacques JF, Lavoie F, Massé E. 2011. Small RNA-induced mRNA degradation achieved through both translation block and activated cleavage. Genes Dev 25:385–396. https://doi.org/10.1101/gad.2001711.
18. Waters LS, Storz G. 2009. Regulatory RNAs in bacteria. Cell 136:615–628. https://doi.org/10.1016/j.cell.2009.01.043.
19. Li W, Ying X, Lu Q, Chen L. 2012. Predicting sRNAs and their targets in bacteria. Genomics Proteomics Bioinformatics 10:276–284. https://doi.org/10.1016/j.gpb.2012.09.004.
20. Storz G, Opdyke JA, Zhang A. 2004. Controlling mRNA stability and translation with small, noncoding RNAs. Curr Opin Microbiol 7:140–144. https://doi.org/10.1016/j.mib.2004.02.015.
21. Gottesman S, Storz G. 2011. Bacterial small RNA regulators: versatile roles and rapidly evolving variations. Cold Spring Harb Perspect Biol 3:a003798. https://doi.org/10.1101/cshperspect.a003798.
22. Gill EE, Chan LS, Winsor GL, Dobson N, Lo R, Ho Sui SJ, Dhillon BK, Taylor PK, Shrestha R, Spencer C, Hancock REW, Unrau PJ, Brinkman FSL. 2018. High-throughput detection of RNA processing in bacteria. BMC Genomics 19:223. https://doi.org/10.1186/s12864-018-4538-8.
23. Taylor PK, Van Kessel ATM, Colavita A, Hancock REW, Mah T-F. 2017. A novel small RNA is important for biofilm formation and pathogenicity in *Pseudomonas aeruginosa*. PLoS One 12:e0182582. https://doi.org/10.1371/journal.pone.0182582.
24. Kay E, Humair B, Dénervaud V, Riedel K, Spahr S, Eberl L, Valverde C, Haas D. 2006. Two GacA-dependent small RNAs modulate the quorum-sensing response in *Pseudomonas aeruginosa*. J Bacteriol 188:6026–6033. https://doi.org/10.1128/JB.00409-06.
25. Janssen KH, Diaz MR, Golden M, Graham JW, Sanders W, Wolfgang MC, Yahr TL. 2018. Functional analyses of the RsmY and RsmZ small noncoding regulatory RNAs in *Pseudomonas aeruginosa*. J Bacteriol 200:e00736-17. https://doi.org/10.1128/JB.00736-17.
26. Wilderman PJ, Sowa NA, FitzGerald DJ, FitzGerald PC, Gottesman S, Ochsner UA, Vasil ML. 2004. Identification of tandem duplicate regulatory small RNAs in *Pseudomonas aeruginosa* involved in iron homeostasis. Proc Natl Acad Sci U S A 101:9792–9797. https://doi.org/10.1073/pnas.0403423101.
27. Sonnleitner E, Prindl K, Bläsi U. 2017. The *Pseudomonas aeruginosa* CrcZ RNA interferes with Hfq-mediated riboregulation. PLoS One 12:e0180887. https://doi.org/10.13.71/journal.pone.0180887.
28. Coleman SR, Smith ML, Spicer V, Lao Y, Mookherjee N, Hancock REW. 2020. Overexpression of the small RNA PA0805.1 in *Pseudomonas aeruginosa* modulates the expression of a large set of genes and proteins, resulting in altered motility, cytotoxicity and tobramycin resistance. mSystems 5:e00204-20. https://doi.org/10.1128/mSystems.00204-20.
29. Wang P, Zhou Z, Hu A, Ponte de Albuquerque C, Zhou Y, Hong L, Sierecki E, Ajiro M, Kruhlak M, Harris C, Guan K-L, Zheng Z-M, Newton AC, Sun P, Zhou H, Fu X-D. 2014. Both decreased and increased SRPK1 levels promote cancer by interfering with PHLPP-mediated dephosphorylation of Akt. Mol Cell 54:378–391. https://doi.org/10.1016/j.molcel.2014.03.007.
30. Bernick EP, Zhang P, Du S. 2010. Knockdown and overexpression of Unc-45b result in defective myofibril organization in skeletal muscles of zebrafish embryos. BMC Cell Biol 11:70. https://doi.org/10.1186/1471-2121-11-70.
31. Aendekerk S, Diggle SP, Song Z, Høiby N, Cornelis P, Williams P, Cámara M. 2005. The MexGHI-OpmD. Multidrug efflux pump controls growth, antibiotic susceptibility and virulence in *Pseudomonas aeruginosa* via 4-quinolone-dependent cell-to-cell communication. Microbiology (Reading) 151:1113–1125. https://doi.org/10.1099/mic.0.27631-0.
32. Breidenstein EBM, de la Fuente-Núñez C, Hancock REW. 2011. *Pseudomonas aeruginosa*: all roads lead to resistance. Trends Microbiol 19:419–426. https://doi.org/10.1016/j.tim.2011.04.005.
33. Barrow K, Kwon DH. 2009. Alterations in two-component regulatory systems of *phoPQ* and *pmrAB* are associated with polymyxin B resistance in clinical isolates of *Pseudomonas aeruginosa*. Antimicrob Agents Chemother 53:5150–5154. https://doi.org/10.1128/AAC.00893-09.
34. Jin Y, Yang H, Qiao M, Jin S. 2011. MexT regulates the type III secretion system through MexS and PtrC in *Pseudomonas aeruginosa*. J Bacteriol 193:399–410. https://doi.org/10.1128/JB.01079-10.
35. Attila C, Ueda A, Wood TK. 2008. PA2663 (PpyR) increases biofilm formation in *Pseudomonas aeruginosa* PAO1 through the *psl* operon and stimulates virulence and quorum-sensing phenotypes. Appl Microbiol Biotechnol 78:293–307. https://doi.org/10.1007/s00253-007-1308-y.
36. Okkotsu Y, Tieku P, Fitzsimmons LF, Churchill ME, Schurr MJ. 2013. *Pseudomonas aeruginosa* AlgR phosphorylation modulates rhamnolipid production and motility. J Bacteriol 195:5499–5515. https://doi.org/10.1128/JB.00726-13.
37. Hunt TA, Peng WT, Loubens I, Storey DG. 2002. The *Pseudomonas aeruginosa* alternative sigma factor PvdS controls exotoxin A expression and is expressed in lung infections associated with cystic fibrosis. Microbiology 148:3183–3193. https://doi.org/10.1099/00221287-148-10-3183.
38. Lizewski SE, Schurr JR, Jackson DW, Frisk A, Carterson AJ, Schurr MJ. 2004. Identification of AlgR-regulated genes in *Pseudomonas aeruginosa* by use of microarray analysis. J Bacteriol 186:5672–5684. https://doi.org/10.1128/JB.186.17.5672-5684.2004.
39. Lizewski SE, Lundberg DS, Schurr MJ. 2002. The transcriptional regulator AlgR is essential for *Pseudomonas aeruginosa* pathogenesis. Infect Immun 70:6083–6093. https://doi.org/10.1128/IAI.70.11.6083-6093.2002.
40. Okkotsu Y, Little AS, Schurr MJ. 2014. The *Pseudomonas aeruginosa* AlgZR two-component system coordinates multiple phenotypes. Front Cell Infect Microbiol 4:82. https://doi.org/10.3389/fcimb.2014.00082.
41. Leoni L, Orsi N, De Lorenzo V, Visca P. 2000. Functional analysis of PvdS, an iron starvation sigma factor of *Pseudomonas aeruginosa*. J Bacteriol 182:1481–1491. https://doi.org/10.1128/JB.182.6.1481-1491.2000.
42. Furman R, Biswas T, Danhart EM, Foster MP, Tsodikov OV, Artsimovitch I. 2013. DksA2, a zinc-independent structural analog of the transcription factor DksA. FEBS Lett 587:614–619. https://doi.org/10.1016/j.febslet.2013.01.073.
43. Murray TS, Ledizet M, Kazmierczak BI. 2010. Swarming motility, secretion of type 3 effectors and biofilm formation phenotypes exhibited within a large cohort of *Pseudomonas aeruginosa* clinical isolates. J Med Microbiol 59:511–520. https://doi.org/10.1099/jmm.0.017715-0.
44. Sangurdekar DP, Zhang Z, Khodursky AB. 2011. The association of DNA damage response and nucleotide level modulation with the antibacterial mechanism of the anti-folate drug trimethoprim. BMC Genomics 12:583. https://doi.org/10.1186/1471-2164-12-583.
45. Minkowski P, Staege H, Groscurth P, Schaffner A. 2001. Effects of trimethoprim and co-trimoxazole on the morphology of *Listeria monocytogenes* in culture medium and after phagocytosis. J Antimicrob Chemother 48:185–193. https://doi.org/10.1093/jac/48.2.185.
46. Amari DT, Marques CNH, Davies DG. 2013. The putative enoyl-coenzyme A hydratase DspI is required for production of the *Pseudomonas aeruginosa* biofilm dispersion autoinducer *cis*-2-decenoic acid. J Bacteriol 195:4600–4610. https://doi.org/10.1128/JB.00707-13.
47. Feinbaum RL, Urbach JM, Liberati NT, Djonovic S, Adonizio A, Carvunis AR, Ausubel FM. 2012. Genome-wide identification of *Pseudomonas aeruginosa* virulence-related genes using a *Caenorhabditis elegans* infection model. PLoS Pathog 8:e1002813. https://doi.org/10.1371/journal.ppat.1002813.
48. Liu L, Li T, Cheng XJ, Peng CT, Li CC, He LH, Ju SM, Wang NY, Ye TH, Lian

M. 2018. Structural and functional studies on. *Pseudomonas aeruginosa* DspI: implications for its role in DSF biosynthesis. Sci Rep 8:3928. https://doi.org/10.1038/s41598-018-22300-1.
49. Petrova OE, Sauer K. 2012. Dispersion by *Pseudomonas aeruginosa* requires an unusual posttranslational modification of BdlA. Proc Natl Acad Sci U S A 109:16690–16695. https://doi.org/10.1073/pnas.1207832109.
50. Potvin E, Lehoux DE, Kukavica-Ibrulj I, Richard KL, Sanschagrin F, Lau GW, Levesque RC. 2003. *In vivo* functional genomics of *Pseudomonas aeruginosa* for high-throughput screening of new virulence factors and antibacterial targets. Environ Microbiol 5:1294–1308. https://doi.org/10.1046/j.1462-2920.2003.00542.x.
51. Haider S, Pal R. 2013. Integrated analysis of transcriptomic and proteomic data. Curr Genomics 14:91–110. https://doi.org/1.0.2174/1389202911314020003.
52. Wang D, Eraslan B, Wieland T, Hallström B, Hopf T, Zolg DP, Zecha J, Asplund A, Li L, Meng C, Frejno M, Schmidt T, Schnatbaum K, Wilhelm M, Ponten F, Uhlen M, Gagneur J, Hahne H, Kuster B. 2019. A deep proteome and transcriptome abundance atlas of 29 healthy human tissues. Mol Syst Biol 15:e8503. https://doi.org/10.15252/msb.20188503.
53. Pain A, Ott A, Amine H, Rochat T, Bouloc P, Gautheret D. 2015. An assessment of bacterial small RNA target prediction programs. RNA Biol 12:509–513. https://doi.org/10.1080/15476286.2015.1020269.
54. Choi K, Kumar A, Schweizer HP. 2006. A 10-min method for preparation of highly electrocompetent *Pseudomonas aeruginosa* cells: application for DNA fragment transfer between chromosomes and plasmid transformation. J Microbiol Methods 64:391–397. https://doi.org/10.1016/j.mimet.2005.06.001.
55. Qiu D, Damron FH, Mima T, Schweizer HP, Yu HD. 2008. P_{BAD}-based shuttle vectors for functional analysis of toxic and highly regulated genes in *Pseudomonas* and *Burkholderia* spp. and other bacteria. Appl Environ Microbiol 74:7422–7426. https://doi.org/10.1128/AEM.01369-08.
56. Busch A, Richter AS, Backofen R. 2008. IntaRNA: efficient prediction of bacterial sRNA targets incorporating target site accessibility and seed regions. Bioinformatics 24:2849–2856. https://doi.org/10.1093/bioinformatics/btn544.
57. Eggenhofer F, Tafer H, Stadler PF, Hofacker IL. 2011. RNApredator: fast accessibility-based prediction of sRNA targets. Nucleic Acids Res 39:W149–W154. https://doi.org/10.1093/nar/gkr467.
58. Tjaden B, Goodwin SS, Opdyke JA, Guillier M, Fu DX, Gottesman S, Storz G. 2006. Target prediction for small, noncoding RNAs in bacteria. Nucleic Acids Res 34:2791–2802. https://doi.org/10.1093/nar/gkl356.